Frequency-Dependent Dielectric and Electrical Characterization of Some Wood Species under Different Conditions: Correlation of Permittivity, Loss Factor, Conductivity, and Impedance

Beytullah Bozali

Dielectric properties of tree samples belonging to Anatolian chestnut, sessile oak, and Scots pine species were measured in the frequency range of 100 Hz to 1 MHz. Test samples were subjected to three different surface conditions, namely control (CW), two-week water-soaked (SW), and two-coat varnish application (VW). The test samples were characterized by analyzing capacitance (*C*), dielectric properties (ε', ε'', and tanδ), AC electrical conductivity (σ_{ac}), normalized conductance (G/ω), and impedance components (Z' and Z''). Frequency analysis revealed that the SW samples exhibited higher *C*, ε', ε'', tanδ, and σ_{ac} values, whereas the VW samples maintained low and stable dielectric properties because of the insulating effect of the varnish layer. The σ_{ac} values reached approximately 10^{-3} S cm^{-1} in the SW samples but remained around 10^{-7} S cm^{-1} in the CW and VW samples, confirming their insulating behavior. In addition, the G/ω and impedance (Z' and Z'') analyses demonstrated distinct electrical responses among the conditioning treatments, with the impedance values following the order VW > CW > SW. These findings provide insights into the dielectric behavior of wood under varying surface conditions. Biologically based dielectric materials could facilitate future advancements in insulation components and moisture-sensitive sensing technologies.

DOI: 10.15376/biores.21.3.8200-8225

Keywords: Dielectric properties; Dielectric energy storage; AC conductivity; Electric modulus; Frequency

*Contact information: Department of Electricity and Energy, Düzce Vocational School, Düzce University, Düzce/Türkiye; *Corresponding author: beytullahbozali@duzce.edu.tr*

INTRODUCTION

The dielectric properties of a non-conducting material define its ability to become polarized under an electric field and, consequently, the extent to which it stores or loses electrical energy. Therefore, the dielectric constant determines its capacity to store energy (James 1975).

For example, changes in permittivity and loss factor have been reported to be of great importance in microwave drying and heat treatment of wood, as higher permittivity and loss factors lead to higher heating rates and better energy efficiency (Şahin and Ay, 2004). Furthermore, changes in electrical conductivity depending on moisture content have been reported to directly influence the performance of wood in practical applications, such as its reliability as an insulating material for power poles and cable trays (James 1975).

This property is particularly important for gate insulators: high permittivity allows more charge carriers to accumulate in the channel region, enabling the device to operate efficiently at lower threshold and operating voltages. Conversely, materials with low dielectric constants can improve carrier mobility by reducing dipolar irregularities that may occur at the semiconductor-insulator interface (Veres *et al.* 2003; Allard *et al.* 2008; Kip *et al.* 2024). Therefore, the selection of materials with high or low dielectric constants, depending on the application requirements, plays a critical role in optimizing device performance. In the literature, different materials such as inorganic compounds, polymer-based systems and hybrid structures containing combinations of these have been investigated and used for the purpose of improving electrical and dielectric properties (Yardım *et al.* 2020; Aydoğmuş *et al.* 2022; Balcı *et al.* 2024; Erbilen Tanrıkulu *et al.* 2024; Güçlü *et al.* 2024). The data provided show the relationship between temperature, humidity, and density, as well as temperature gradient and absence of woody trees and vegetation (Saeed 2022). Another study revealed the relationship between thermal conductivity and electrical conductivity in 47 wood samples and wood products, confirming its use in the study of building materials (Saeed *et al.* 2022). The freezing behavior of water in wood was investigated using dielectric spectroscopy, and temperature and cooling rate were found to have a significant effect on permittivity and loss factor. This further illustrates the sensitivity of wood permittivity to environmental conditions (Ai *et al.* 2024).

Chai *et al*. (2025) conducted a study based on experimental and numerical analysis to investigate the effects of temperature and humidity on the dielectric properties of wood veneers and to model the frequency-dependent behavior of the dielectric under high-frequency heating. Wood is a material capable of exhibiting high permittivity due to its complex and heterogeneous structure. Experimental correlations between frequency-dependent dielectric parameters and thermal conductivity of multilayer building materials were evaluated to assess the energy performance of building envelopes using dielectric methods (Said *et al*. 2024).

Investigations that were conducted through cavity perturbation and Microwave Thermogravimetric Analysis (MW-TGA) revealed that the driving effect of dielectric properties on the reaction kinetics, in particular, microwave-induced formation significantly increased the conversion efficiency (Luo *et al.* 2017). Measurements in the frequency (397 to 2985 MHz) and temperature (25 to 700 °C) ranges performed on different biomass types (straw, grass, bark, wood chips and fiber waste) revealed that significant changes occurred in the dielectric constant (ε'), loss (ε'') and tanδ values, especially during the drying, pyrolysis, and biochar formation stages. Yao *et al*. (2025) also stated that biochar addition improved electromagnetic energy absorption and thermal conversion efficiency by increasing tanδ up to 400 °C (Yao *et al.* 2025). Also, within the scope of microwave-assisted pyrolysis applications, the dielectric responses formed during the thermal conversion process of thick wood blocks were found to be directly related to the energy absorption and the degree of conversion. The obtained results showed that the complex dielectric permittivity changed significantly depending on the conversion process and that the energy transfer efficiency was directly related to the dielectric properties (Vorhauer-Huget *et al*. 2024). The dielectric behavior of wood-reinforced epoxy composites with different fiber ratios (5%, 10%, 15%, 20%) and chemical modifications (NaOH, K_2CO_3) in the frequency range of 100 Hz to 2 MHz was analyzed, and the effect of fiber amount and frequency on orientation and interfacial polarization was investigated in detail. An increase in fiber ratio increases the dielectric constant, especially at low and medium frequencies, while this contribution decreased at high frequencies, and chemical modification suppresses the polarization behavior (Jayamani *et al.* 2021). A new method developed for *in situ* thermal transmittance measurement has confirmed the strong correlation between the dielectric constant and thermal conductivity of wood and wood-based materials. The findings indicate that the energy performance of building shells can be estimated quickly and accurately with frequency-based dielectric measurements (Saeed *et al.* 2022). It has been determined that the dielectric constants of delignified cellulose-based materials subjected to oxidation process, measured in the frequency range of 10^3–10^7 Hz, are significantly higher than those of untreated samples. As the crystal structure weakens with increasing oxidation time, the dielectric constant increases and tanδ decreases. These results provide an important theoretical and experimental basis for the engineering applications of wood-based dielectric materials (Xu *et al.* 2025). Frequency-based measurements of the piezoelectric response of wood materials demonstrate a direct relationship between the obtained V_{rms} values and the texture density, moisture content, and degree of crystallinity of the material. Stronger piezoelectric signals were observed in highly textured and knotty regions, clearly demonstrating the decisive role of frequency in these responses (Özan 2025).

There are dielectric studies in the literature on different wood species [pine (*Pinus sylvestris* L.) by Kol (2009), fir (*Abies nordmanniana*), and oak (*Quercus petraea*) by Kol and Yalçın (2015), poplar (*Populus deltoids* cv. I-69/55) by He *et al.* (2017), *Pinus sylvestris* var. *mongolica* by Xu *et al.* (2019), and kayu malam (*Diospyros blancoi*), keranji (*Dialium indum*), and kumpang (*Myristica cinnamomea*) by Jayamani *et al*. (2020)].

The main objective of this study was to characterize the frequency-dependent dielectric and electrical responses of Anatolian chestnut, sessile oak and Scots pine by measuring capacitance (C) and conductance (G/ω), dielectric permittivity (ε' and ε''), dielectric loss tangent (tanδ), AC conductivity (σ_{ac}), and impedance components (Z' and Z'') over the frequency range of 100 Hz to 1 MHz under DC bias voltages ranging from 0 to 100 V for three conditioning conditions (CW, SW, and VW).

These wood species have different characteristics. The sapwood of Scots pine varies from yellowish white to pink. It darkens gradually over time due to weathering. Its specific gravity has been reported as 0.49 g/cm^3 (Şanıvar and Zorlu 1980). It is relatively light and soft wood with abundant resin. It is used as construction timber, in joinery, furniture, packaging material, and in box and basket making (Hammond *et al*. 1969). Anatolian chestnut wood is hard, compact, and flexible. It has abundant tannin. The outer wood is off-yellow, sometimes white or gray. Its air-dried specific gravity is 0.56 g/cm^3. It is used in bridge and pier piers, joinery, furniture production, and lathe work. The specific gravity of sessile oak wood is 0.86 g/cm^3. It is used in barrels, wagons, veneer, furniture manufacturing, and the sides of boats and bridges. The color of this tree is off-white. The sapwood is dark. The annual rings are prominent (Şanıvar and Zorlu 1980).

Measurements in the frequency range from 100 Hz to 1 MHz give us a better understanding of how surface treatment parameters and internal structure parameters (density, multivariate properties focusing on parameters such as specific heat, normalized conductance, AC conductivity and dielectric response) contribute to the field of electromagnetic fields. Microwave drying, energy storage, electrical sensing and bioelectronic components. The aim of this study was to determine the frequency-dependent electrical and resistive properties of wood materials under different surface conditions to contribute to the development of clean technologies.

EXPERIMENTAL

In this study, Anatolian chestnut (*Castanea sativa* Mill.), sessile oak (*Quercus petraea* (Matt.) Liebl.) and Scots pine (*Pinus sylvestris* L.) woods were used.

The test samples used in the study consisted of test samples that have been dried and kept in a closed environment for at least 20 years. Air conditioning procedures were performed on the test specimens (ISO 1976). Table 1 shows the test dimensions of the wood samples.

Table 1. Test Measurements of Wood Samples

Wood Type	(CW) (mm × mm × mm)	(SW) (mm × mm × mm)	(VW) (mm × mm × mm)
Anatolian chestnut	500 × 80 × 15	250 × 80 × 15	250 × 80 × 15
Sessile oak	500 × 65 × 15	250 × 65 × 15	250 × 65 × 15
Scots pine	500 × 95 × 15	250 × 95 × 15	250 × 95 × 15

The experimental design was established as follows. CW test specimens consisted of wood test specimens without any treatment.

Prior to measurements, SW test samples were soaked in water for two weeks to ensure complete water saturation. Measurements were performed as is, without drying the SW test samples. Before evaluation, the samples were continuously monitored to maintain their saturation state and to ensure visualization and repeatability of dielectric measurements.

A solvent-based, transparent, glossy wood varnish was used for the VW test specimens (colorless; viscosity: 13 to 17 s, determined with a DIN Cup No. 4 at 20 °C; relative density: 0.83 to 0.87 g/cm³; touch dry: 1 to 3 h; recoating interval: 12 h; complete drying time: 12 h). Prior to application, the surfaces were completely cleaned of oil stains, sawdust, and old paint and varnish residue. They were prepared dry and lightly sanded. Two varnish coats were applied to the surfaces, with a 12-h interval between coats. Varnishing was performed in accordance with ASTM D3023-98 (2017) standard.

The measurements were subjected to 100 Hz to 1 MHz and 0 to 100 V DC bias. Table 1 shows the CW, SW, VW, ε', ε'', tan δ, σ_{ac}, G/ω values geometry-normalized with the actual A and t of the samples. CW samples were prepared at L = 500 mm, while SW/VW samples are prepared by cutting to L = 250 mm. All samples have the same thickness (t = 15 mm), and a constant, masked effective electrode area (A_{eff}) was used in the measurements. The equation $Z_n = Z\,A/t$ (Ω m) was used for impedance comparisons. The general trend: Z'/Z'': VW > CW > SW; σ_{ac}: SW ≈ 10^{-3} S, CW≈VW ≈ 10^{-7} S. The length differences in Table 1 are process-provided, and the results have been made comparable by normalization.

Electric Field

The electric field is defined as the force acting on a unit positive charge. The electric field is a vectorial physical quantity. The mathematical relation for the electric field is shown in Eq. 1.

$$\vec{E} = \frac{\vec{F}}{q} \quad (1)$$

Equation 1, $\vec{F}$ represents the electric force acting on the charge, and q represents the test charge.

Figure 1 shows the dipole orientation of a dielectric material under the influence of an electric field. Figure 1a shows that when no external electric field is applied, the dipoles within the dielectric are randomly oriented, thus no net polarization occurs. However, Fig. 1b shows that when an external electric field ($E_{applied}$) is created by applying a potential difference across the ends of the material, the dipoles within the dielectric begin to align in the direction of this field.

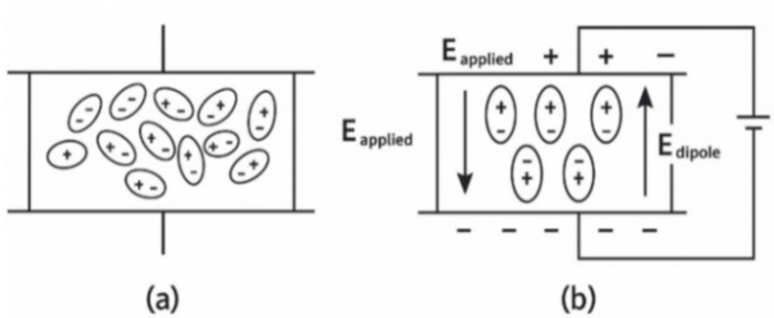

Fig. 1. Orientation of dipoles according to electric field intensity (Tinga and Nelson 1973; Vaydoğan 2017).

In Fig. 1, under the influence of the external electric field, the molecular dipoles within the dielectric are oriented, resulting in a dipole-induced electric field (E_{dipole}) in the opposite direction to the applied field. Polarization (P) occurs as the charges within the material rearrange, resulting in a decrease in the net electric field. Equation 2 gives the polarization equation.

$$P = \varepsilon_0 X_e E \quad (2)$$

In Eq. 2, P represents polarization, ε_0 represents the permittivity of the space, X_e represents the electrical susceptibility, and E represents the applied electric field (Bozkurt 1982).

When examining the direct current (DC) properties of wood, when completely dry, wood exhibits high electrical resistance, acting as a good insulator. However, as humidity increases, especially at moisture contents below the fiber saturation point, the resistance decreases rapidly due to ionic conductivity. Humidity increases from 0% to 30% can increase electrical conductivity by approximately 10^6 times. This increase occurs quite rapidly up to the point of fiber saturation; after this point, the increase in conductivity is more limited. At room temperature, the relationship between the electrical resistivity of wood and moisture content can be expressed logarithmically (Stamm 1927; Bozkurt 1982).

The properties of wood materials under alternating current (AC), including their conductivity, were quite low at high frequencies. The AC resistance of dry wood was approximately 10 x 10^6 Ω cm, corresponding to a conductivity approximately a billion times lower than that of direct current (DC). At a moisture content of 10 to 12%, the DC resistance decreased to approximately 1/1000 of its dry value. Fiber orientation had a significant effect on conductivity; under AC, the resistance perpendicular to the grain was 3 to 3.5 times higher than the resistance parallel to the grain. Furthermore, as the moisture content increased from 0% to 25%, alternating current resistance reaches much lower values compared to direct current resistance (Bozkurt 1982).

The Measurement of Dielectric Properties

To perform dielectric spectroscopy (DS) measurements, two opposite surfaces of the test specimens were electrode using copper conductive tape approximately 20 mm wide. The appearance of the prepared test specimen is shown in Fig. 2A. As shown in Fig. 2A, contact zones approximately 10 mm wide were created on two opposite surfaces of the test specimen to allow for the connection of the LCR meter probes. Copper conductive tapes applied to two opposite surfaces of the test specimen caused it to behave in a parallel plate capacitor geometry, enabling the determination of its dielectric properties under an alternating electric field. The experimental setup used for dielectric measurements is shown in Fig. 2B.

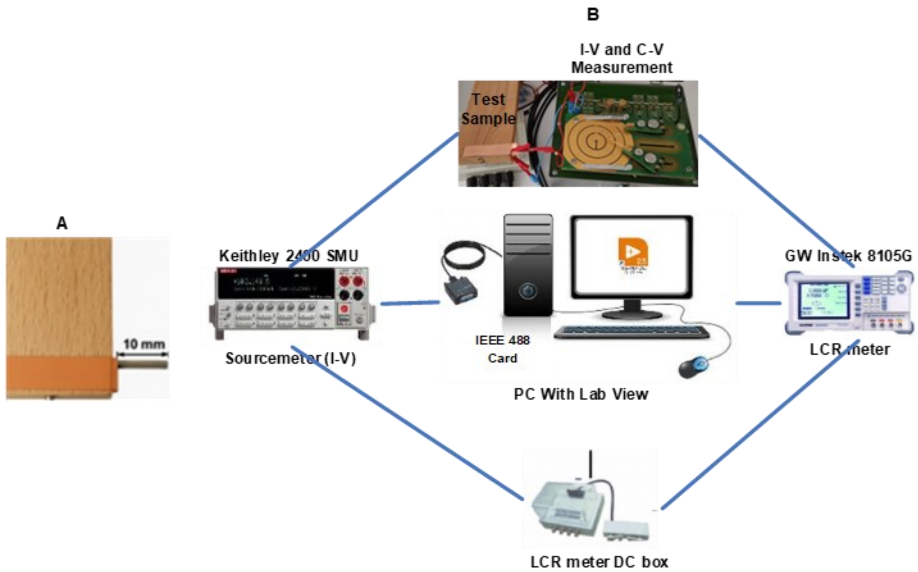

Fig. 2. Image of the test sample (A); and DS measurement system used in the study (Demir *et al.* 2024; İbrahimoğlu *et al.* 2024; Ramazanoğlu *et al.* 2025) (B)

The DS measurement system, shown in Fig. 2, acts as a source meter and a current generator when different electric field values are applied to the contacts of the test samples. The LCR measuring device applies a low-amplitude AC signal to the contacts of the test samples for dielectric characterization. The synchronization between the experimental and test systems is checked for accuracy with the help of an oscilloscope placed at the connection points. A GW Instek 8105G LCR measuring device capable of measuring in the frequency range between 20 Hz and 5 MHz is used to measure and record the electrophysical parameters (İbrahimoğlu *et al.* 2024). Dielectric property measurements are carried out with the help of an impedance analysis system consisting of a Keithley 2400 SMU and a GW Instek 8105G LCR meter, which operates with a computer-controlled IEEE 488 interface card (Demir *et al.* 2024; Ramazanoğlu *et al.* 2025).

In this study, the dielectric properties of Anatolian chestnut, sessile oak, and Scots pine trees were investigated. All obtained values were scaled logarithmically, and graphs were drawn. Dielectric parameters can be calculated using the following formulas:

$$C = C_0 \varepsilon' \quad (3)$$

$$\frac{G}{w} = C_0 \varepsilon'' \quad (4)$$

In Eqs. 3 and 4, ε' and ε'' denote the real and imaginary components of the dielectric constant, while *C* refers to the specific heat capacity of the system. Capacitance (*C*) and normalized conductance (G/ω) are key frequency-dependent dielectric parameters for characterizing the electrical behavior of materials (Kip *et al.* 2024; Kırkbınar *et al.* 2024). The parameter G/ω reflects processes such as conductivity losses, polarization relaxation, and segmental mobility, which are intrinsically related to the imaginary dielectric constant (ε''). As expressed in Eq. 4, *G* represents conductivity (S), $\omega = 2\pi f$ is the angular frequency (rad/s), $C_0=\varepsilon_0 \cdot A/d$ corresponds to the geometric capacitance, and ε'' indicates the dielectric loss factor (Macdonald 1992; Barsoukov and Macdonald 2005; Demir 2025).

Equation 5 can be used to express the complex impedance (Z^*) to form Eqs. 6–9 (Gencel *et al.* 2024; İbrahimoğlu *et al.* 2024; Kip *et al.* 2024; Demir 2025; Wei *et al.* 2016):

$$Z^* = Z' + jZ'' \tag{5}$$

The complex dielectric constant ε^* can be expressed using the impedance spectrum as in Eq. 6:

$$\varepsilon^* = \frac{1}{jwZ^*} = \varepsilon' + j\varepsilon'' \tag{6}$$

In Eq. 6, ε^* represents the complex permittivity and $\omega = 2\pi f$ represents the angular frequency. Using Eq. 6, the real ε' and imaginary ε'', complex dielectric constant components can be calculated as follows. (Türk *et al.* 2020; Kocakülah and Köysal 2023).

$$\varepsilon' = \frac{1}{wC_0} \cdot \frac{Z''}{(Z')^2 + (Z'')^2} \tag{7}$$

$$\varepsilon'' = \frac{1}{wC_0} \cdot \frac{Z'}{(Z')^2 + (Z'')^2} \tag{8}$$

$$C_0 = \varepsilon_0 \frac{A}{d} \tag{9}$$

In Eqs. 7 to 9, C_0 represents the capacitance of free space, while in Eq. 9, the value of ε_0 = 8.854 × 10^{-12} F/m, represents the dielectric permittivity (Kocakülah and Köysal 2023). In Eq. 9, *A* represents the effective electrode area in contact with the electrodes, and *d* represents the thickness of the composite sample (Demir 2025).

The alternating current (AC) electrical conductivity (σ_{ac}) is determined from dielectric loss using Eq. 10, where the parameter *G* represents the conductance dissipated by the system under an external electric field and its conversion into heat.

In Eq. 10, ε_0 is the permittivity of free space (8.854 × 10^{-12} F/m), ω is the angular frequency, and ε'' is the imaginary component of the dielectric permittivity.

$$\sigma_{ac}(w) = \varepsilon_0 w \varepsilon'' \tag{10}$$

In Eq. 11, *A* is a constant, *s* is an exponential expression that determines conductivity behavior as a function of frequency. The conductivity of the system ε'' varies with frequency. High electrical conductivity indicates that charge transfer is facilitated, leading to increased dielectric energy losses. Conversely, low conductivity values suggest higher electrical resistance of the material. Furthermore, it may indicate that the material has insulating properties, thus increasing its capacity to store electrical energy (Macdonald 1992; Barsoukov and Macdonald 2005; Demir 2025).

$$\sigma_{ac} = A.w^{s} \quad (11)$$

The loss tangent (tanδ) is defined as the ratio of the imaginary permittivity (ε'') to the real permittivity (ε') of the complex dielectric permittivity ($\varepsilon^* = \varepsilon' - j\varepsilon''$), as expressed in Eq. (12) (Demir 2025; Ramazanoğlu *et al.* 2025).

$$\tan\delta = \frac{\varepsilon''}{\varepsilon'} \quad (12)$$

The complex impedance (Z^*) was calculated using Eq. (13), while the real (Z') and imaginary (Z'') impedance components were determined using Eqs. (14) and (15), respectively.

$$Z^* = \frac{1}{i\omega C_0 \varepsilon^*} = Z' + jZ'' \quad (13)$$

$$Z' = \frac{\varepsilon''}{\omega C_0 \left[\varepsilon'^2 + \varepsilon''^2 \right]} \quad (14)$$

$$Z'' = \frac{\varepsilon'}{\omega C_0 \left[\varepsilon'^2 + \varepsilon''^2 \right]} \quad (15)$$

Equations (13)-(15) were used to program the impedance measurement from the dielectric constant measurements (Demir *et al.* 2024; Ramazanoğlu *et al.* 2025, Ramazanoğlu *et al.* 2025).

Comparative Dielectric Properties of Wood and Alternative Materials for Applications

To highlight the practical importance of the dielectric parameters investigated in this study (C, ε', ε'', tanδ, σ_{ac}, G/ω, Z', and Z''), the electrical behavior of wood is compared with that of other materials used in sensor applications. Table 2 shows that wood stands out for its renewability, low cost, and biocompatibility.

Table 2. Comparison of Dielectric Properties and Sensing Potential of Wood and Other Materials

Material Type	Dielectric Constant (ε')	Loss Factor (tan δ)	Advantages	Limitations	References
Wood	2 to 20 (depending on MC); >1000 at high MC	0.01 to 0.10	Renewable, low-cost, biocompatible	Sensitive to moisture and environment	(Şahin and Ay 2004; Xu *et al.* 2019)
Polymer-based composites	4 to 40	0.01 to 0.05	Lightweight, processable, tunable properties	Limited thermal stability, aging effect	(Elloumi *et al.* 2021)
Ceramics (e.g., $BaTiO_3$, PZT)	500 to 5000	0.02 to 0.10	Very high ε, stable performance	Brittle, high cost	(Barsoukov and Macdonald 2005)
Polymer–ceramic hybrids	50 to 200	0.01 to 0.05	Combination of flexibility and high ε	Complex processing, higher cost	(Wu *et al.* 2022; Zha *et al.* 2021)

While polymer-based composites, ceramics, and hybrid systems offer higher permeability or stability, they often suffer from limitations such as brittleness and high cost (Şahin and Ay 2004; Xu *et al*. 2019; Elloumi *et al*. 2021; Barsoukov and Macdonald 2005; Wu *et al.* 2022; Zha *et al.* 2021).

RESULTS AND DISCUSSION

The capacitance C_0 and conductivity (G/w) of the composite medium are expressed as a function of frequency by Eqs. 2 and 3. In Eqs. 3 and 4, (C) is the capacitance, G is the conductivity, $\omega=2\pi f$ is the angular frequency, (ε') is the real dielectric constant (energy storage), (ε'') is the imaginary dielectric constant (energy loss), and $C = \varepsilon_0\varepsilon_r A/d$ is the geometric capacitance. The dielectric constants are ε_0 and ε_r (Wei *et al.* 2016; Demir 2025). Equations 3 and 4 help to understand the variation of properties such as specific heat capacity (C) with frequency, and the frequency-dependent behavior of (C) can be indirectly related to the variation of ε' and ε'' (Kao 2004).

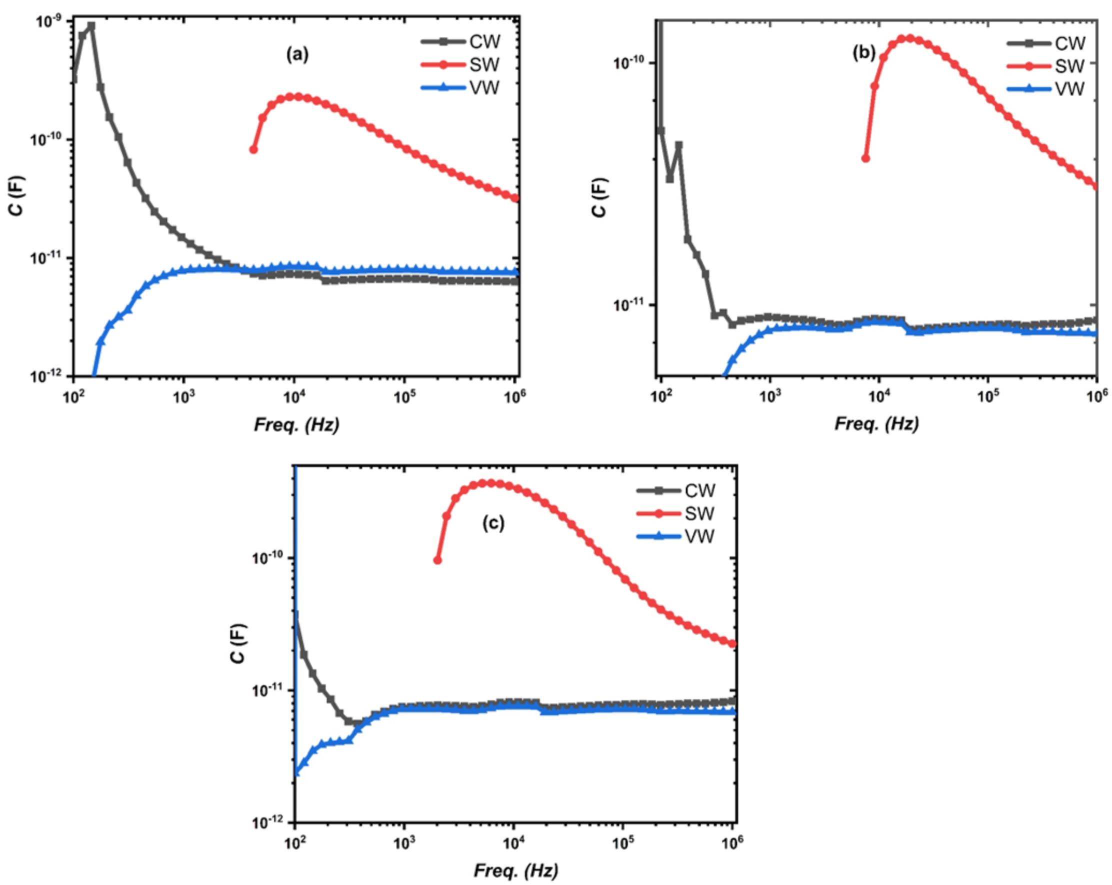

Fig. 3. Capacitance-frequency variation for a) Anatolian chestnut, b) sessile oak, and c) Scots pine

Equation 12 defines the loss factor (tanδ), which represents the dielectric losses of the material. Higher tanδ values indicate increased energy losses, while lower tanδ values indicate better insulation performance (Kao 2004; Barsoukov and Macdonald 2005).

The *C–F* graph in Fig. 3 shows the variation of specific heat capacities (*C*) with frequency measured under three different surface conditions (CW, SW and VW) for a) Anatolian chestnut, b) sessile oak and c) Scots pine test samples.

As seen from Eqs. 3 and 4, specific capacitance (*C*) is a parameter affected by dielectric permittivity (ε' and ε''), sample geometry, and electrical conductivity Ondo-Ndong *et al*. (2018) reported that the decrease in capacitance values observed in materials is inversely proportional to the increase in conductivity values.

The *C–F* graph shown in Fig. 3 reveals that the dielectric response of Anatolian chestnut samples changed significantly depending on the surface conditions. The continuous wave (CW) specimen exhibited high capacitance values, approximately ~10^{-9} F, in the low frequency range (~100 Hz), and these values decreased rapidly with increasing frequency. This situation is due to the Maxwell-Wagner-Sillars (MWS) type of interfacial polarization created by different material structures. The SW specimen showed a clear resonant peak in the mid-frequency range (~10^4 Hz). This peak is due to the entrance of water molecules into the wood pores, which increases the dipole alignment and ionic conductivity. The relatively high (ε) value can be attributed to the contribution of water to the current. This is also emphasized by previous studies showing that the dielectric constant of wood increases with increasing moisture content due to the high permeability of water (Şahin and Ay 2004; Xu *et al.* 2019).

As shown in Fig. 3, the capacitance (*C*) of all wood species generally decreased with increasing frequency. The CW samples showed higher capacitance at low frequencies, followed by a gradual decrease at higher frequencies. The SW samples exhibited a distinct capacitance peak in the intermediate frequency region, approximately between 10^3 and 10^4 Hz, which may be associated with enhanced interfacial polarization caused by absorbed water. In contrast, the VW samples had the lowest and most stable capacitance values over the measured frequency range, indicating that the varnish layer limited charge accumulation and dipole polarization. Overall, water treatment increased the dielectric response, whereas varnish application reduced the capacitance by restricting charge transport. Similar trends were reported by Zhou *et al.* (2013), who showed that increasing moisture content increased the capacitance and dielectric properties of medium-density fiberboard, especially at low frequencies. Saeed *et al.* (2022) also emphasized the relationship between moisture-related dielectric behavior and the electrical response of wood-based materials.

In Fig. 4, the behavior of three different test samples, a) Anatolian chestnut, b) sessile oak, and c) Scots pine, and the dielectric constant real permittivity (ε') corresponding to frequencies between 100 Hz and 1 MHz are analyzed in detail. The complex impedance method, commonly used in dielectric analysis, can be used to calculate the properties of materials based on the dielectric constant of the dielectric material. Although the dielectric constant showed a similar frequency-dependent structure in all experiments, it can be observed that there was a large difference between ambient conditions and measurements. Based on the Anatolian chestnut data in Fig. 4a, the CW test sample reached very high values of $\varepsilon' \approx 10^3$ at low frequencies (~100 Hz), and (ε') decreased logarithmically as frequency increased. This indicates intense interfacial polarization and indicates the accumulation of free charge carriers within the material. In the SW test samples, the ε' value reached a significant maximum at medium frequencies (10^3 to 10^4 Hz), exhibiting resonant characteristics. This suggests that the dipole contribution of water molecules activated mobile charge carriers. In VW samples, the ε' value was lower (~10^2) and it remained approximately constant with frequency. This indicates that the varnish layer suppressed the electrical polarization, limiting the dielectric response of the material. In the graph of the sapwood oak in Fig. 4b, the ε' value of the CW sample at low frequency was about 10^2, and this value decreased with increasing frequency. This indicates that the polarization process is limited by frequency due to the dense structure of the sapwood oak. The value of the SW sample increased significantly between 10^3 and 10^4 Hz, reaching a maximum at this point (about 10^2) and then decreasing. This indicates that the interaction with water also induced a resonant-type polarization mechanism in the oak. The VW test sample showed a stable graph with low and stable ε' values (~10). These test samples were determined to exhibit passive behavior against the electric field, operating at their insulation limits. Figure 4c shows a schematic representation of a Scots pine sample for the CW test, where ε' started at low frequencies 10^2 to 10^3 and then stabilized at higher frequencies. This suggests that the fiber structure of Scots pine allows for polarization by the effective charge at low frequencies. The SW sample showed a resonance effect, with ε' peaking around 10^3 to 10^4 Hz. This indicates that the dielectric response of wood increased with moisture absorption. The VW sample showed remarkably stable and low ε' values (~ 10). This confirms the effect of varnish application in maintaining dynamic polarization in all wood species.

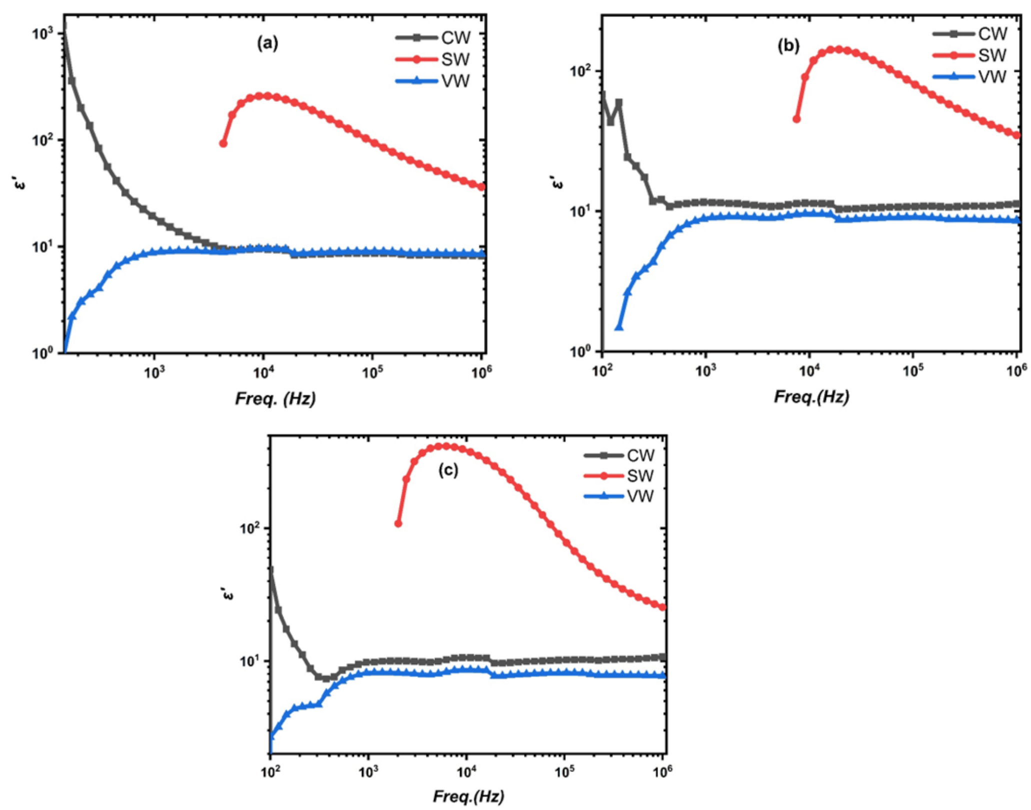

Fig. 4. Frequency-dependent behavior of the real dielectric permittivity for a) Anatolian chestnut, b) sessile oak, and c) Scots pine

The frequency-dependent behavior (ε') is therefore very sensitive to the microstructural characteristics of the wood species and the surface treatment used. The resonant peaks, especially those observed in the SW test samples, indicate the activation of ion mobility and dipolar processes in the wood material. The stable and low (ε') values observed in the VW test samples indicate that the electrical insulation effect can be achieved. Frequency-dependent measurements of the actual dielectric constant (ε') reveal that the electrical properties of wood species depend directly on physical parameters such as moisture absorption capacity, surface layer conductivity, fiber structure, and density.

In the study conducted by Pentoś *et al.* (2016), the dielectric properties of the wood species sweet cherry, Roth birch, oak, ash, European larch, Scotch pine, and Norway spruce were determined depending on the frequency and grain orientation of the wood. Measurements for samples cut from heartwood and sapwood were carried out at frequencies ranging from 1 kHz to 1 MHz, parallel and perpendicular to the visible grain. It was concluded that ε' and tanδ were affected by frequency and anisotropy. The effect of wood species on ε' and tanδ was observed in the entire frequency range. However, significant differences were reported between wood species for ε' below 5 kHz and for tanδ below 200 kHz. In general, higher relative permittivity and loss coefficient values were determined in hardwoods than in softwoods. While ε' decreased with increasing frequency, tanδ increased at frequencies above 200 kHz for all wood species, regardless of fiber orientation. These observations agree with the findings of Pentoś *et al.* (2017).

Şahin and Ay (2004) measured the dielectric properties at 9.8 GHz and 2.45 GHz for three hardwood species: European larch, poplar, alder, and oriental beech. Measurements performed using the Von Hippel transmission line method revealed similar dielectric behavior in all wood types under 0 to 28% moisture content and three different fiber orientations. It was reported that dielectric properties increased with increasing moisture content, and fiber orientation had a significant effect on these properties.

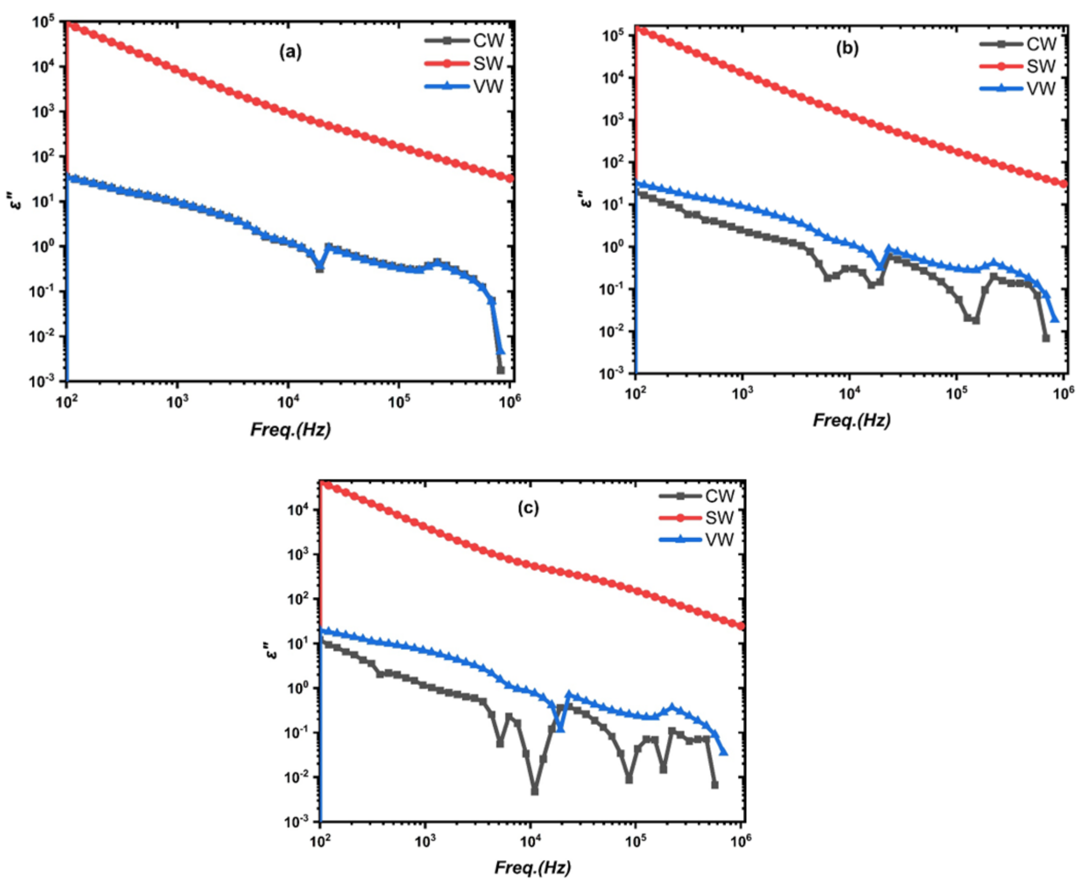

Fig. 5. Frequency-dependent behavior of the imaginary permittivity for a) Anatolian chestnut, b) sessile oak, and c) Scots pine

The ε''–F graph presented in Fig. 5 provides comparative dielectric loss behaviors of CW, SW, and VW test samples of Anatolian chestnut, sessile oak, and Scots pine species, considering the imaginary dielectric permittivity (ε'') values measured in the frequency range of 100 Hz to 1 MHz. Real permittivity (ε') represents the energy storage capacity of the system, while the (ε'') value reflects the energy loss under the applied alternating electric field, *i.e.*, the portion of the system converted to heat. In dielectric constant calculations based on complex impedance parameters, the (ε'') value is defined by Eq. 8.

In Fig. 5a, the ε'' values for Anatolian chestnut data, particularly for SW test samples, remained logarithmically high across the entire frequency range; this indicates increased conductivity and dielectric losses due to the high dipole of water molecules. In the case of SW tests, the value (ε'') decreased to 105, indicating the presence of water in the mixture. In the case of CW and VW samples, a decrease in shear modulus (ε'') value with increasing sample thickness was observed. According to the VW analysis, the value (ε'') indicates that the adsorption decreases the ion mobility and charge transfer rate. Figure 5b shows that the imaginary permittivity (ε'') of sessile oak decreased with increasing frequency for all conditioning conditions. The SW sample exhibited the highest ε″ values, whereas the VW sample maintained the lowest and most stable values throughout the measured frequency range. This behavior indicates that absorbed water enhanced dielectric losses, while the varnish layer suppressed charge transport and interfacial polarization.

Figure 5c shows that the elastic modulus (ε'') of Scots pine, especially in the CW and VW tests, showed a large variation. These changes can be explained by environmental factors, such as bacterial contamination and pesticide exposure. However, higher values (ε'') were observed for the SW samples, indicating that the Scotch pine had a higher water absorption capacity and higher ionic strength.

Therefore, the increase observed for all specimens in the SW test indicates that an increase in water content significantly increased the dielectric loss. This highlights the importance of proper treatment of wood products to maintain their thermoelectric properties. On the other hand, the small values of ε'' for the VW measurements indicate that the static phase was affected by the surface layer. These results demonstrate the excellent performance of surface adsorption under different flow conditions.

James (1975) found that white oak and Douglas oak have similar properties in the frequency range of 20 Hz to 50 MHz, in the temperature range of -20 to +90 °C, and in electrical conductivity. The permittivity increased with increasing moisture content or temperature and decreased with increasing frequency. Values ranged from approximately 2.0 for cold, dry material at high frequencies to approximately 1 million for hot, immersed wood at low frequencies. The loss tangent was noted to exhibit maximum and minimum values under different conditions. The frequencies at which extreme values were observed were generally higher with increasing moisture content or temperature. The loss tangent was found to range from about 0.01 to about 100.

Avramidis (2016) investigated the dielectric properties of various softwood species at different moisture contents, temperatures, and frequencies ranging from 0.1 to 30 MHz. The results showed that the loss factor increased with increasing moisture content and temperature and decreased with increasing frequency. Furthermore, it was reported that the loss factor values measured in the longitudinal direction were higher than those measured in the radial direction.

The *G*/*ω*–*F* graph is shown in Fig. 6. Frequency-dependent variation of normalized conductance (G/ω) in the frequency range of 100 Hz to 1 MHz for (a) Anatolian chestnut, (b) sessile oak, and (c) Scots pine under three conditioning conditions (CW, SW, and VW).

Figure 6 shows the energy loss experienced by the test samples under the influence of an external alternating electric field and the degree to which this energy is converted into heat.

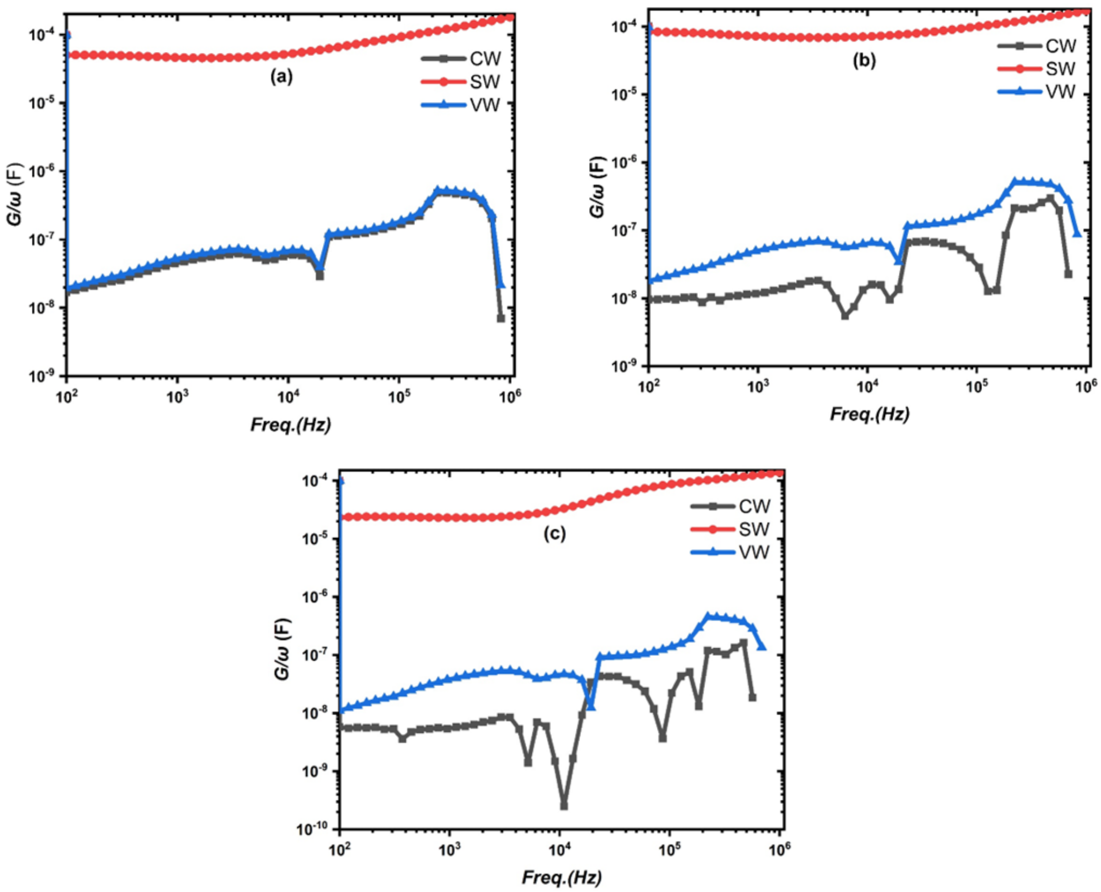

Fig. 6. Frequency-dependent conductance *G*/*ω*–*F* graph for a) Anatolian chestnut, b) sessile oak, and c) Scots pine

In Fig. 6a, the SW test sample of Anatolian chestnut wood reached the highest *G*/*ω* values over a wide frequency range, and dielectric loss was quite pronounced. This suggests that water molecules diffuse into the wood matrix, increasing conductivity and contributing to polarization. The CW and VW test samples exhibited lower and relatively flat *G*/*ω*–*F* graph, suggesting lower ionic mobility and a more insulating structure.

Figure 6b shows that the *G*/*ω*–*F* graph of the sessile oak SW test specimen remained high, remaining constant particularly in the low-frequency region and increasing slightly towards higher frequencies. In the VW test specimen, it was determined that water absorption was limited by the surface barrier effect, and therefore the *G*/*ω*–*F* graph remained at moderate levels. The CW specimen exhibited low normalized conductance at low frequencies, suggesting enhanced insulating behavior.

Figure 6c shows that Scots pine exhibited relatively low normalized conductance under all surface conditions. This can be attributed to the natural structural fiber arrangement and resin content of Scots pine. However, the sharp jumps observed as frequency increased in the VW test sample indicated frequency-sensitive polarization behavior of the varnish layer. The damping at low frequencies in the CW test sample indicated limited mobility of the matrix. The SW test sample, on the other hand, maintained a lower *G*/*ω*–*F* graph compared to other species.

The energy transfer rate can be expressed as tan*δ*, energy loss. The value of tan*δ* is an important parameter that determines the electrical conductivity of the system under fault conditions. This is an important indicator for evaluating the performance of power systems in power conversion applications. The loss factor, tan*δ*, is a parameter that describes how much energy a dielectric material loses. The tan*δ*-*F* graph, shown in Fig. 7, compares the dielectric loss performance of three different CW, SW, and VW test specimens: a) Anatolian chestnut, b) sessile oak, and c) Scots pine, over the frequency range of 100 Hz to 1 MHz.

Figure 7a shows that the tan*δ* value in Anatolian chestnut reached a lower value of 102, especially in the VW test samples. This indicates that the surface modification increased energy loss by increasing the dipole orientation and surface polarization. The CW and SW test samples exhibited low tan*δ*, indicating poor polarization loss and dielectric behavior. The lower tan*δ* in the SW test sample indicates that the air reduced the dipole rotation and reduced the energy dissipation.

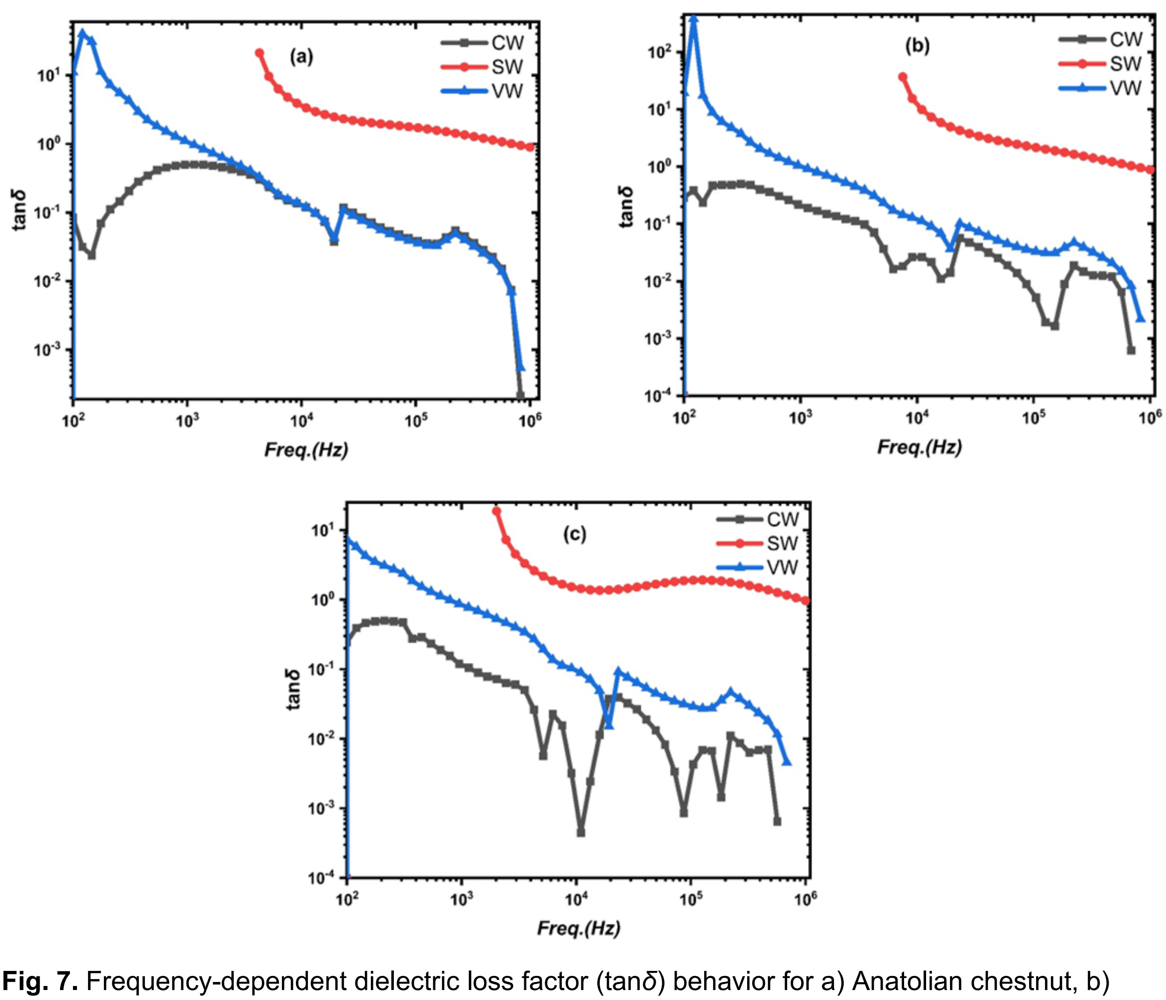

Fig. 7. Frequency-dependent dielectric loss factor (tan*δ*) behavior for a) Anatolian chestnut, b) sessile oak, and c) Scots pine

Figure 7b shows a similar pattern for the stagnant oak. The VW test sample recorded high tanδ values in the frequency range, indicating that the varnish layer improved the interfacial polarization by increasing the surface roughness. The lowest loss factor value was obtained in the SW test sample, indicating that the electrical behavior is more pronounced in cold environments.

The value of tanδ of the CW specimen was relatively stable due to its unique fiber structure and water content. Figure 7c shows that tanδ values initially decreased with increasing frequency. The loss of the VW signal was highest in the frequency range of 10^3 to 10^5 Hz. This increase can be explained by an increase in global polarization and the effects of global energy neutralization mechanisms. The value of tanδ of the SW specimen was also lower, and the dielectric constant was higher. Therefore, although VW specimens exhibited a higher loss rate at lower frequencies, this was related to the surface charge density, dipole moment, and polarization effects. In contrast, the hydrophobic nature decreased tanδ due to hydrophobic effects. These results suggest that tanδ is an important discriminating factor, especially in high-intensity applications, considering energy loss, stability, and selectivity. The energy loss in dielectric systems under different electric fields is determined by the value of tanδ and not only by the charge storage properties of the system but also by its energy conversion efficiency.

Elloumi *et al.* (2021) studied the dielectric properties of wood–plastic composites (WPCs) using dielectric spectroscopy, to analyze their interaction with electromagnetic fields, and to evaluate their applications in new applications. The dielectric properties of WPCs were monitored continuously from 1 MHz to 1 GHz. The WPCs were fabricated using extrusion and compression molding with different types of wood and wood fibers, high-density polyethylene, and 3% maleated polyethylene. The results indicated that wood fibers altered the resistivity of polyethylene at low frequencies. However, they noted that there was no effect on microwave frequencies. They stated that increasing the fiber content improved the dielectric properties of the composites.

Figure 8 shows the (σ_{ac}–F) graph for the AC electrical conductivity behavior of three different CW, SW, and VW test samples, a) Anatolian chestnut, b) sessile oak, and c) Scots pine, in the frequency range of 100 Hz to 1 MHz. The AC electrical conductivity (σ_{ac}) equations are expressed in Eqs. 11 and 12. Alternating current electrical conductivity (σ_{ac}) refers to a material's ability to carry charge under an alternating electric field. High σac values indicate increased charge transfer and energy losses, while low (σ_{ac}) values indicate better insulation properties and electrical stability (Macdonald 1992; Barsoukov and Macdonald 2005; Demir 2025).

Figure 8a shows that the SW specimen of Anatolian chestnut exhibited the highest AC electrical conductivity (σ_{ac}), with values on the order of 10^{-3}S cm^{-1} over the investigated frequency range. This behavior indicates that absorbed water enhanced ionic conduction and charged transport within the wood structure. In contrast, the CW and VW specimens exhibited significantly lower σ_{ac} values, approximately 10^{-8} to 10^{-7} S cm^{-1} and 10^{-7} to 10^{-6} S cm^{-1}, respectively, particularly at low frequencies. The lower conductivity of the VW specimen suggests that the varnish layer acted as an electrical barrier, restricting transport charge and reducing the overall electrical conductivity.

A similar trend was observed for the sessile oak specimens (Fig. 8b). The SW specimen exhibited the highest AC electrical conductivity (σ_{ac}), with values on the order of 10^{-3} S cm^{-1}, whereas the CW and VW specimens showed lower conductivities, generally between 10^{-7} and 10^{-6} S cm^{-1} at low frequencies. The fluctuations observed in the VW specimen at intermediate, and high frequencies may be associated with interfacial polarization and frequency-dependent charge transport.

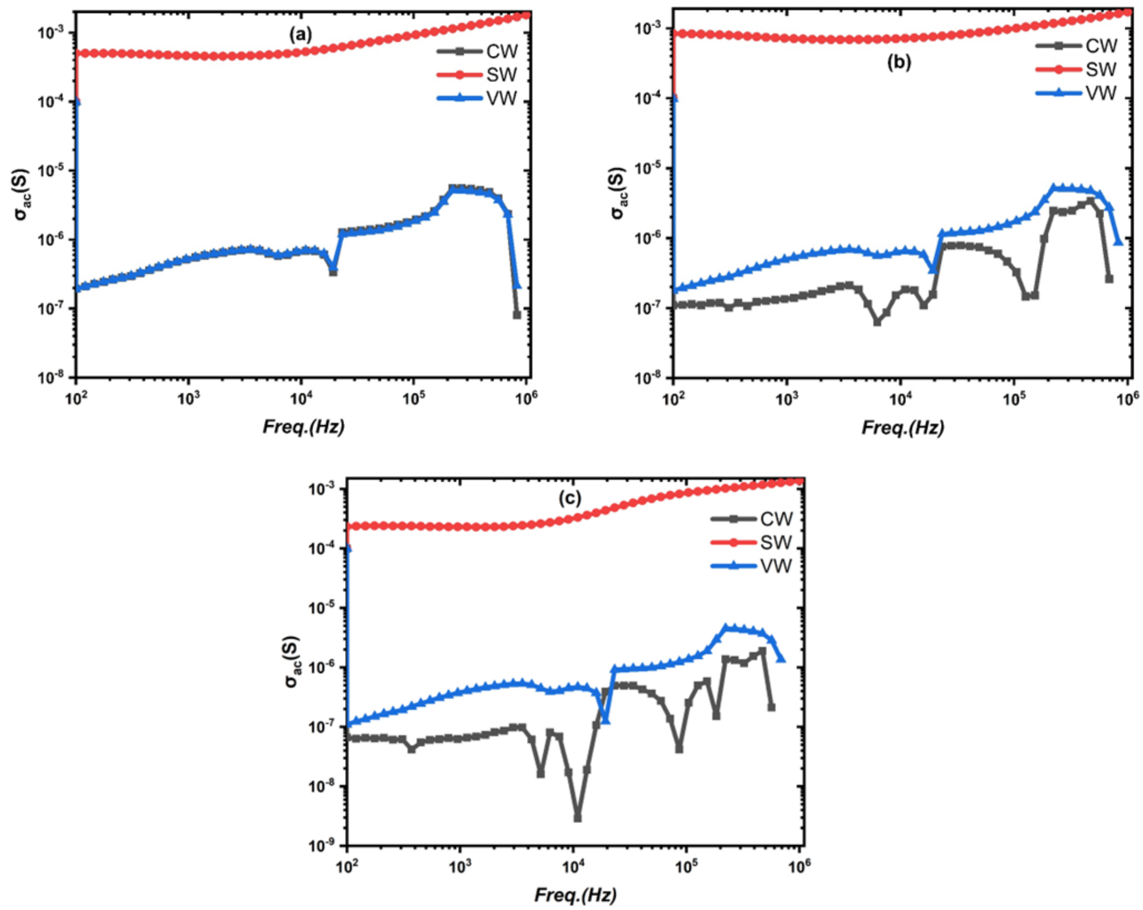

Fig. 8. Frequency-dependent variation of AC electrical conductivity for a) Anatolian chestnut, b) sessile oak, and c) Scots pine

Figure 8c shows that the SW Scots pine specimens exhibited the highest AC electrical conductivity (σ_{ac}) over the investigated frequency range. In contrast, the VW specimens showed lower conductivity with slight fluctuations at intermediate, and high frequencies, whereas the CW specimens exhibited the lowest σac values, reaching approximately 10^{-8} S cm^{-1} at low frequencies. The higher conductivity observed in the SW specimens may be attributed to enhanced ionic conduction resulting from absorbed moisture, while the varnish layer likely restricted charge transport, leading to lower σ_{ac} values.

Figure 9 shows the (Z'–F) graph for the real impedance behavior of three different CW, SW, and VW test samples, a) Anatolian chestnut, b) sessile oak, and c) Scots pine, in the frequency range of 100 Hz to 1 MHz. Figure 9 shows the real impedance (Z') behavior of Anatolian chestnut, sessile oak, and Scots pine wood species, obtained under three different surface conditions (CW, SW, and VW) and in the frequency range of 100 Hz to 1 MHz. The parameter Z^* is the complex impedance and is given in Eq. 13. The value of Z^* can be related to the real and imaginary impedance (Z' and Z''). The real and imaginary impedance (Z' and Z'') values are calculated as in Eqs. (14) and (15).

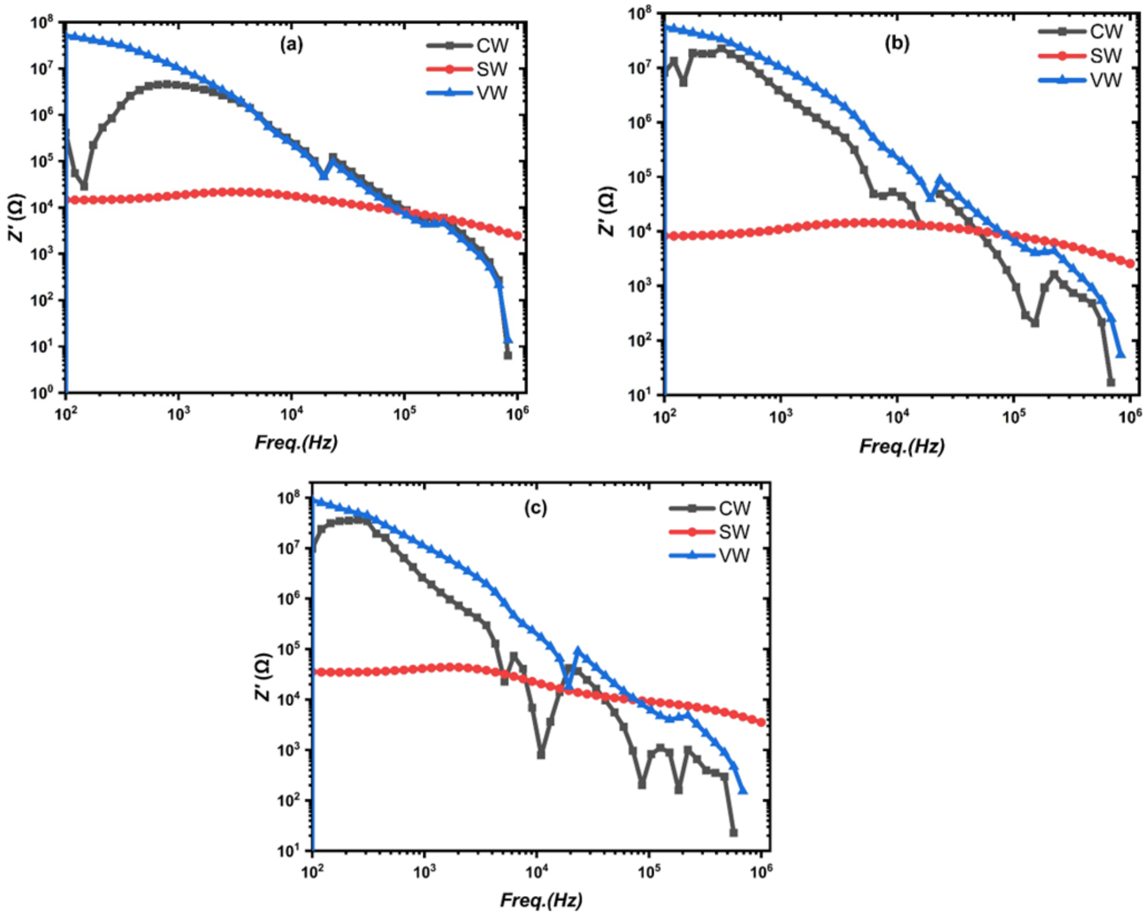

Fig. 9. The real impedance (*Z*′) for a) Anatolian chestnut, b) sessile oak, and c) Scots pine

For all three species, VW consistently exhibited the highest (*Z*′) values, indicating better insulation due to the suppression of ion transport. In contrast, the liquid wave samples immersed in water had the lowest and flatter profiles (*Z*′), increasing the ionic conductivity at saturation temperature. The CW control samples fell between the two extremes and showed a monotonic decrease in (*Z*′) with increasing frequency. Scots pine exhibited step-like features indicating multiple relaxation processes associated with its heterogeneous microstructure.

These findings are consistent with studies in literature highlighting the strong influence of moisture and surface modification on the dielectric and impedance properties of wood (James 1975; Zelinka *et al.* 2007; Pentoś *et al.* 2016).

Figure 10 shows the (*Z*″–*F*) graph of the imaginary impedance behaviors of Anatolian chestnut, sessile oak, and Scots pine wood species obtained under three different surface conditions (CW, SW, VW) and in the frequency range of 100 Hz to 1 MHz. The value of *Z** can be related to the real and virtual impedance (*Z*′ and Z″). The real and virtual impedance (*Z*′ and *Z*″) values are calculated as in Eqs. (14) and (15).

For all three species, varnished samples (VW) exhibited the highest (*Z*″) values, indicating stronger polarization and energy storage resulting from surface insulation. In contrast, water-immersed samples SW exhibited the lowest and flattest (*Z*″) profiles, reflecting the dominance of ionic conductivity under saturated conditions. The specimen showed a moderate pattern of reduction (*Z*″), and Scots pine showed distinct morphological characteristics (*Z*″) with distinct grain and cell sizes. The present results are consistent with previous studies. The combination reduces the contribution of the resistance change, while the surface roughness and contrast increase the polarization-related contributions (James 1975; Pentos *et al.* 2016).

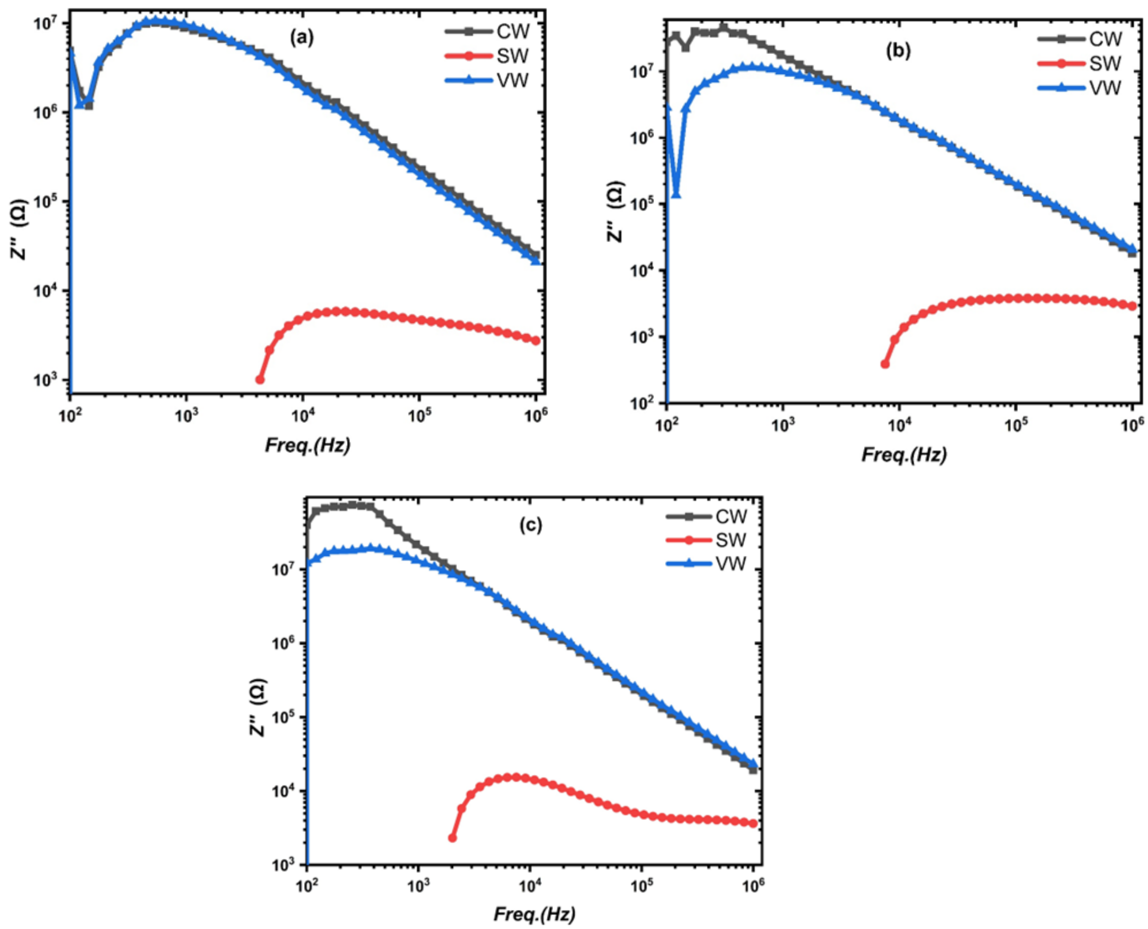

Fig. 10. The imaginary part of impedance (Z'') for a) Anatolian chestnut, b) sessile oak, and c) Scots pine

In Figs. 9 and 10, the absolute values (Z') and values (Z'') were obtained at different points in the VW model, which indicate good shielding and adaptive capacity, respectively. The SW plot shows that these values were higher for the ionic concentrations of these compounds. The CW test model remained in the middle, showing a steady and increasing behavior. Adsorption occurs with *Z'* and *Z'* ions. Different degrees of degradation of Scotch oak were observed in the Vernin samples, possibly due to their different species and characteristics.

A holistic evaluation of Figs. 3 to 10 and Table 3 shows that the order VW > CW > SW was consistent for (Z') and (Z'') in all species, and that the varnish coating increased (Z'/Z'') by increasing interfacial polarization and capacitive storage. SW, on the other hand, reduced both (Z') and (Z'') values due to saturated ionic transport, flattening the spectra.

While σ_{ac} showed high and stable levels reaching ≈10^{-3} S in SW, it maintained its insulating character by staying at ≈10^{-7} S in CW and VW. C and ε' were highest in SW and lowest in VW, while (ε'') and tanδ showed increased losses in SW. The G/ω data supported energy distribution in the resonance/intermediate frequency regions. Anatolian chestnut exhibited strong capacitive behavior with pronounced Cole–Cole arcs under varnish, while sessile oak exhibited weaker relaxation tendencies. Table 3 indicates that moisture and surface conditioning are the primary factors determining the dielectric/impedance response of wood.

Table 3. Electrical and Dielectric Properties of Wood Types

Wood Type	Condition	*C* (F)	*ε′* (real)	*ε″* (imag.)	tan *δ*	σ_{ac}	*G*/*ω*	*Z′*, *Z″*
Anatolian chestnut	SW	Highest	Highest	Highest	High	≈10^{-3} S	High/flat	Lowest,
	CW	Medium	Medium	Medium	Medium	≈10^{-7} S	Medium	Intermediate
	VW	Lowest	Lowest	Low–medium	Low–medium	≈10^{-7} S	Medium–high	Highest
Sessile oak	SW	Highest	Highest	Highest	High	≈10^{-3} S	High/flat	Lowest
	CW	Medium	Medium	Medium	Medium	≈10^{-7} S	Medium	Intermediate
	VW	Lowest	Lowest	Low–medium	Low–medium	≈10^{-7} S	Medium–high	Highest
Scots pine	SW	Highest	Highest	Highest	High	≈10^{-3} S	High/flat	Lowest
	CW	Medium	Medium	Medium	Medium	≈10^{-7} S	Medium	Intermediate
	VW	Lowest	Lowest	Low–medium	Low–medium	≈10^{-7} S	Medium–high	Highest

In a study by Zelinka *et al*. (2007), electrical impedance spectra (EIS) were obtained for southern pine wood equilibrated to a moisture content of 12%. Cylindrical graphite electrodes were embedded in the wood nearly end-on along a line parallel to the grain, and the EIS properties were characterized as functions of the interelectrode distance and electrode contact pressure over the frequency range of 0.1 Hz to 300 kHz. Relaxation time was found to be sensitive to electrode contact pressure but relatively insensitive to the interelectrode distance (Martin *et al.* 2015). The EIS distribution width is sensitive to the interelectrode distance but not to contact pressure. Initially, the data suggested a finite contact resistance between the wood and the electrode, but further investigation revealed that the "contact resistance" was an artifact due to electrode edge effects.

Tiitta *et al.* (2020) combined electrical impedance spectroscopy (EIS) with machine learning algorithms to determine the proportion of heartwood in pine chips and bark in birch chips. Measurements were performed over the frequency range of 42 Hz to 5 MHz, and the KNN, DT, and SVM algorithms were used for classification. Using EIS combined with the KNN algorithm, classification accuracies of 91% for pure samples, 73% for pine heartwood, and 64% for birch bark in mixed samples were achieved.

Martin *et al*. (2015) observed significant differences in the obtained complex impedance spectra for beech, oak, basswood, poplar, amaranth, ebony, mahogany, rosewood, zebrawood, African birch, ebony, and sandalwood. Processing of the obtained low-frequency impedance spectra reportedly yielded integrated parameters. Comparison of the integrated parameters with the average pore diameter determined separately for tropical wood species revealed clear correlations.

CONCLUSIONS

1. An attempt was made to determine the frequency-dependent dielectric/electrical properties of Anatolian chestnut, sessile oak and Scots pine under three conditioning conditions (CW, SW, VW). The results showed that both the structural properties of the wood species and surface modifications had decisive effects on parameters such as ε', ε'', tanδ, σ_{ac}, C, G/ω, Z', and Z''. SW test samples showed significant dielectric losses and high AC conductivity due to the high ion mobility and dipole polarization provided by increased moisture content, which could make them attractive for electromagnetic absorber and sensor applications.
2. When considering the use of SW in insulation/dielectric elements, it was found that high conductivity and increased losses can suppress Z'/Z'', increasing the risk of leakage and stability. Because VW exhibited lower losses and a more stable capacitive response, it can be said to offer potential for use cases requiring low leakage and stable capacitive performance. With its low loss factor and stable insulation behavior, VW test samples can be said to be suitable for high voltage insulation and surface protection systems.
3. The hierarchy VW > CW > SW was confirmed for the impedance components across all species and conditions. In the SW case, σ_{ac} ≈10^{-3} S indicates ionic transport, while CW/VW ≈10^{-7} S indicates the insulating regime. While C and ε' peaked in the SW, broad-band losses of ε'' and tanδ were observed to increase. VW increased Z'/Z'' in the test samples and stabilized capacitive storage. The G/ω curves supported energy dissipation in the transition regions. At the species level, varnished chestnut showed distinct Cole–Cole arcs, Scots pine shows multiple relaxation traces due to heterogeneous structure, and oak shows fainter relaxation trends. This indicates that the frequency-dependent dielectric/impedance response can be distinctly tuned by humidity conditioning and surface coating, making VW suitable for applications requiring low leakage and stable capacitive performance, while SW can be used for conductivity-oriented applications such as humidity sensing.

ACKNOWLEDGMENTS

I would like to thank Prof. Dr. Nevzat Çakicier for his help in providing the wooden material for this study and Assoc. Prof. Dr. Ahmet Demir for providing laboratory facilities for determining the measurements made on the experimental materials.

REFERENCES CITED

ASTM D3023-98, (2017). "Standard practice for determination of resistance of factory-applied coatings on wood products to stains and reagents," *ASTM International*.

Ai, M., Gao, S., Song, X., and Feng, M. (2024). "Evaluation of the effects of temperature and cooling rate on the freezing of water in wood using dielectric spectroscopy," *Wood Science and Technology* 58, 589-608. https://doi.org/10.1007/s00226-024-01550-5

Allard, S., Forster, M., Souharce, B., Thiem, H., and Scherf, U. (2008). "Organic semiconductors for solution-processable field-effect transistors (OFETs)," *Angewandte Chemie - International Edition* 47(22), 4070-4098. https://doi.org/10.1002/anie.200701920

Avramidis, S. (2016). "Dielectric properties of four softwood species at lowlevel radio frequencies for optimized heating and drying," *Drying Technology* 34(7), 753-760, https://doi.org/10.1080/07373937.2015.1072719

Aydoğmuş, E., Yılmaz, E., and Demir, A. (2022). "Life cycle assessment and characterization of tincal ore reinforced polyester and vinylester composites," *Journal of the Turkish Chemical Society Section B: Chemical Engineering* 5(2), 183-194.

Balcı, E., Vahid, A. F., Avar, B., and Altındal. (2024). "On a detail examination of frequency and voltage dependence of dielectric, electric modulus, ac conductivity (σac) of the Al/DLC/p-Si structures between 2 kHz and 1 MHz," *Physica B: Condensed Matter* 695(416576), 1-9. https://doi.org/10.1016/j.physb.2024.416576

Barsoukov, E., and Macdonald, J. R. (2005). *Impedance Spectroscopy: Theory, Experiment, and Applications*, 2nd Ed., Hoboken, NJ, USA: Wiley-Interscience.

Bozkurt, Y. (1982). "Ağaç Teknolojisi (Wood Technology)," *İstanbul Üniversitesi Orman Fakültesi Yayınları* 2839(296).

Chai, Y., Lin, X., Du, G., Zhou, Q., Tu, D., and Hu, C. (2025). "Heat transfer and temperature distribution of manufacturing laminated veneer lumber using high-frequency heating: Finite element simulation and experimental validation," *Construction and Building Materials* 479(141437), 1-10. https://doi.org/10.1016/j.conbuildmat.2025.141437

Demir, A. (2025). "Multispectral analysis of photosensitive perovskite-E7 liquid crystal composites: Correlating optical response with electrical properties," *Optical Materials* 162(January), 1-10. https://doi.org/10.1016/j.optmat.2025.116878

Demir, A., Musatat, A. B., and Kip, Ş. Z. (2024). "Investigation of dielectric anisotropy and electrical modulus-impedance properties of PCBM/E7 composite for organic electronic devices applications," *Celal Bayar Üniversitesi Fen Bilimleri Dergisi*, 21(2), 72-79. https://doi.org/10.18466/cbayarfbe.1562667

Elloumi, I., Koubaa, A., Kharrat, W., Bradai, C., and Elloumi, A. (2021). "Dielectric properties of wood–polymer composites: Effects of frequency, fiber nature, proportion, and chemical composition," *Journal of Composites Science* 5(6), 141, 1-11. https://doi.org/10.3390/jcs5060141

Erbilen Tanrıkulu, E., Güçlü, Ç. Ş., Altındal, Ş., and Durmuş, H. (2024). "A high sensitivity temperature coefficient of the Au/n-Si with (CdTe-PVA) structure based on capacitance/conductance-voltage (C/G-V) measurements in a wide range of temperature," *Measurement: Journal of the International Measurement Confederation* 238(115316), 1-9. https://doi.org/10.1016/j.measurement.2024.115316

Gencel, O., Musatat, A. B., Demir, A., Tozluoğlu, A., Tutuş, A., Kıllı, U., Fidan, H., and Kosovalı Cavuş, F. (2024). "Transforming industrial byproduct to eco-friendly functional material: Ground-granulated blast furnace slag reinforced paper for renewable energy storage," *Science of the Total Environment* 954(December 2023), 1-15. https://doi.org/10.1016/j.scitotenv.2024.176616

Güçlü, Ç. Ş., Ulusoy, M., and Altındal, Ş. (2024). "A comparison electrical characteristics of the Au/(pure-PVA)/n-Si and Au/(CdTe doped-PVA)/n-Si (MPS) type Schottky structures using I–V and C–V measurements," *Journal of Materials Science: Materials in Electronics* 35(12), 1-10. https://doi.org/10.1007/s10854-024-12650-0

Hammond, J. J., Donnelly, E. T., Harrod, W. F., Rayner, N. A., and Özden, F. (1969). "Ağaç işleri teknolojisi, Mesleki ve Teknik Öğretim Kitapları", İrfan Zorlu (ed.), Ajans Türk Matbaacılık Sanayi, 554 pages.

He, X., Xie, J., Xiong, X., Li, Y., Wei, Y., Quan, P., Mou, Q., and Li, X. (2017). "Study on dielectric properties of poplar wood over an ultra-wide frequency range," *BioResources* 12(3), 5984-5995. https://doi.org/10.15376/biores.12.3.5984-5995

İbrahimoğlu, E., Demir, A., Çalışkan, F., and Tatlı, Z. (2024). "The dielectric characteristics of spray deposited α-Si3N4:ZnO thin films: The nitride effect on frequency-dependent capacitance and conductance profiles," *Solid State Sciences* 158(July), article 107754. https://doi.org/10.1016/j.solidstatesciences.2024.107754

ISO 554. (1976). "Standard atmospheres for conditioning and/or testing," *International Standardization Organization,* Geneva, Switzerland.

James, W. L. (1975). "Dielectric properties of wood and hardboard: Variation with temperature, frequency, moisture content, and grain orientation," *Department of Agriculture* Forest Service, Forest Products Laboratory.

Jayamani, E., Mohammed Saleh Al Mzrouie, A., Hari Prashanth, P. V. S., and Jeyanthi, S. (2021). "Effect of chemical treatments on polarization and dielectric properties of Kumpang wood reinforced epoxy composite," *Materials Today: Proceedings* 46, 8887-8894. https://doi.org/10.1016/j.matpr.2021.05.606

Jayamani, E., Rahman, M. R., Hamdan, S., Kyari, M. I., Bakri, M. K. Bin, Sanaullah, K., and Khan, A. (2020). "Dielectric properties of natural borneo woods: Keranji, kayu malam, and kumpang elammaran," *BioResources* 15(4), 7815-7827.

Kao, K. C. (2004). *Dielectric Phenomena in Solids*, 1st Ed. Amsterdam, Netherlands: Elsevier Academic Press.

Kao, K. C. (2004). *Dielectric Phenomena in Solids, With Emphasis on Physical Concepts of Electronic Processes*, 1st Ed., Elsevier Academic Press, Amsterdam, Netherlands. https://doi.org/10.1016/B978-0-12-396561-5.50019-0

Kip, Ş. Z., Gegin, K., Demir, A., Köysal, O., Öztürk, S., and Kösemen, A. (2024). "The novel n-channel liquid crystal organic field effect transistor (LC-n-OFET): A promising technology for low-power electronics," *Organic Electronics* 125(106965), 1=8. https://doi.org/10.1016/j.orgel.2023.106965

Kırkbınar, M., İbrahimoglu, E., Demir, A., and Çalışkan, F. (2024). "Investigating ultra-thin rGO coated ZnO core-shell structures in MOS devices: Electrical/dielectric characteristics and relaxation mechanism," *Materials Science and Engineering: B*, 310(117722), 1-9. https://doi.org/10.1016/j.mseb.2024.117722

Kocakülah, G., and Köysal, O. (2023). "Conductivity and optical bandgap parameters variations of methyl red-doped 4-pentyl-4′-cyanobiphenyl nematic liquid crystal: Norland optical adhesive 65 photopolymer composites," *Journal of Materials Science: Materials in Electronics* 34(19), 1-11. https://doi.org/10.1007/s10854-023-10857-1

Kocakülah, G., and Köysal, O. (2023). "The fluorescent materials effect on physical parameters of nematic liquid crystals," *Journal of Electronic Materials* 52(8), 5707-5718. https://doi.org/10.1007/s11664-023-10522-7

Kol, H. Ş. (2009). "Thermal and dielectric properties of pine wood in the transverse direction," *BioResources* 4(4), 1663-1669. https://doi.org/10.15376/biores.4.4.1663-1669

Kol, H. Ş., and Yalçın, İ. (2015). "Predicting wood strength using dielectric parameters," *BioResources* 10(4), 6496-6511. https://doi.org/10.15376/biores.10.4.6496-6511

Luo, H., Bao, L., Kong, L., and Sun, Y. (2017). “Low temperature microwave-assisted pyrolysis of wood sawdust for phenolic rich compounds: Kinetics and dielectric properties analysis,” *Bioresource Technology* 238, 109-115. https://doi.org/10.1016/j.biortech.2017.04.030

Macdonald, J. R. (1992). “Impedance spectroscopy,” *Annals of Biomedical Engineerin*, 20, 289-305. https://doi.org/10.1166/jnn.2011.5092

Martin, T., Nordsiek, S., and Weller, A. (2015). "Low-frequency impedance spectroscopy of wood," *Journal of Research in Spectroscopy* 1, 1-9. https://doi.org/10.5171/2015.910447

Ondo-Ndong, R., Essone-Obame, H., Moussambi, Z. H., and Koumba, N. (2018). “Capacitive properties of zinc oxide thin films by radiofrequency magnetron sputtering,” *Journal of Theoretical and Applied Physics* 12(4), 309-317. https://doi.org/10.1007/s40094-018-0309-9

Özan, Z. E. (2025). *Odunun Piezoelektrik Özellikleri ile Elektriksel Potansiyelin Dikili Ağaçlardaki Değişimi ve Fizyolojik Özelliklerine Olan Etkisinin Belirlenmesi* (Determination of piezoelectric properties of wood and changes in electrical potential in planted trees and their effects on physiological properties), in: *T.C. Bartın Üniversitesi Lisansüstü Eğitim Enstitüsü, Orman Endüstri Mühendisliği Anabilim Dalı,* Doktora Tezi, Bartın, 2025 (pp. 1-223).

Pentoś, K., Łuczycka, D., and Wysoczański, A. (2016). “The use of complex impedance as a parameter for wood differentiation,” *Wood Research* 61(1), 13-24.

Pentoś, K., Łuczycka, D., and Wysoczański, T. (2017). Dielectric properties of selected wood species in Poland. *Wood Research, 62*(5), 727–736.

Ramazanoğlu, D., Subaşı, A., Musatat, A. B., Demir, A., Subaşı, S., and Maraşlı, M. (2025). “Dielectric property enhancement of glass fiber-reinforced concrete via TiO_2 nanocomposites,” *Structures* 79(109444), 1–16. https://doi.org/10.1016/j.istruc.2025.109444

Ramazanoğlu, D., Subaşı, A., Musatat, A. B., Demir, A., Subaşı, S., and Maraşlı, M. (2025). “Multifunctional SnO_2-@ doped glass fiber-reinforced concrete: Improved microstructure, mechanical, dielectric, and energy storage characteristics,” *Construction and Building Materials* 476, article 141231. https://doi.org/10.1016/j.conbuildmat.2025.141231

Saeed, N. (2022). “Experimental data for thermal conductivity and dielectric properties of wood and wood-based materials,” *Data in Brief* 42, article 108027. https://doi.org/10.1016/j.dib.2022.108027

Saeed, N., Malen, J. A., Chamanzar, M., and Krishnamurti, R. (2022). “Experimental correlation of thermal conductivity with dielectric properties of wood and wood-based materials: Possibilities for rapid in-situ building energy evaluation,” *Journal of Building Engineering* 50, article 104178. https://doi.org/10.1016/j.jobe.2022.104178

Saeed, N., Malen, J. A., and Krishnamurti, R. (2024). “Predicting effective thermal conductivity of multilayered assemblies related to wood-frame construction based on dielectric properties: Data exploration for application to rapid in-situ building energy evaluation,” *Construction and Building Materials* 447, article 138102. https://doi.org/10.1016/j.conbuildmat.2024.138102

Stamm, A. J. (1927). “The electrical resistance of wood as a measure of its moisture content, ” *Industrial & Engineering Chemistry* 19, 1021-1025.

Sugimoto, H., Takazawa, R., and Norimoto, M. (2005). “Dielectric relaxation due to heterogeneous structure in moist wood,” *Journal of Wood Science* 51(6), 549-553.

https://doi.org/10.1007/s10086-004-0688-1

Şahin, H., and Ay, N. (2004). "Dielectric properties of hardwood species at microwave frequencies," *J. Wood Science* 50(5), 375-380. https://doi.org/10.1007/s10086-003-0575-1

Şanıvar, N., and Zorlu, İ. (1980). "Ağaç işleri gereç bilgisi temel ders kitabı, Mesleki ve Teknik Öğretim Kitapları, Milli Eğitim Basımevi, İstanbul, Turkey, Etüd ve Programlama Dairesi Yayınları No: 43, 472 pages.

Tiitta, M., Tiitta, V., Heikkinen, J., Lappalainen, R., and Tomppo, L. (2020). "*Classification of wood chips using electrical impedance spectroscopy and machine learning*," Sensors, 20(4), 1076. https://doi.org/10.3390/s20041076

Tinga, W., and Nelson, S. (1973). "Dielectric properties of materials for microwave processing-tabulated," *Journal of Microwave Power* 8(1), 23-65. https://doi.org/10.1080/00222739.1973.11689017

Türk, Ç. G., Tan, S. O., Altındal, Ş., and İnem, B. (2020). "Frequency and voltage dependence of barrier height, surface states, and series resistance in Al/Al_2O_3/p-Si structures in wide range frequency and voltage," *Physica B: Condensed Matter* 582(411979), 1-7. https://doi.org/10.1016/j.physb.2019.411979

Vaydoğan, K. G. (2017). *Isıl Işlem Görmüş Bazı Ağaç Malzemelerin Farklı Rutubet Şartlarındaki Isı Iletkenlik Ve Dielektrik Özelliklerinin Belirlenmesi (Determination of Thermal Conductivity and Dielectric Properties of Some Heat-Treated Wood Materials Under Different Moisture Conditions)*, Karabük Üniversitesi, Fen Bilimleri Enstitüsü Orman Endüstri Mühendisliği, Yüksel Lisans Tezi, Karabük.

Veres, J., Ogier, S. D., Leeming, S. W., Cupertino, D. C., and Khaffaf, S. M. (2003). "Low-k insulators as the choice of dielectrics in organic field-effect transistors," *Advanced Functional Materials* 13(3), 199-204. https://doi.org/10.1002/adfm.200390030

Vorhauer-Huget, N., Seidenbecher, J., Bhaskaran, S., Schenkel, F., Briest, L., Gopalkrishna, S., Barowski, J., Dernbecher, A., Hilfert, L., Rolfes, I., and Dieguez-Alonso, A. (2024). "Dielectric and physico-chemical behavior of single thermally thick wood blocks under microwave assisted pyrolysis," *Particuology* 86, 291-303. https://doi.org/10.1016/j.partic.2023.07.004

Wei, L., Liu, Q. X., Zhu, B., Liu, W. J., Ding, S. J., Lu, H. L., Jiang, A., and Zhang, D. W. (2016). "Low-cost and high-productivity three dimensional nanocapacitors based on stand-up ZnO nanowires for energy storage," *Nanoscale Research Letters* 11(213), 1-9. https://doi.org/10.1186/s11671-016-1429-2

Wu, H., Li, J., Shen, Z., Wang, Y., and Zhou, W. (2022). "Polymer/ceramic-based dielectric composites for energy storage and conversion," *Energy & Environmental Materials* 5(6), article e12237. https://doi.org/10.1002/eem2.12237

Xu, C., Chai, H., Cao, T., Cai, M., Cai, Y., and Liu, H. (2019). "Detection of dielectric constant of Pinus sylvestris Var. mongolica and its influencing factors," *BioResources* 14(2), 4532-4542. https://doi.org/10.15376/biores.14.2.4532-4542

Xu, H., Qiu, F., Han, W., Liu, J., and Xue, Z. (2025). "Study of the effect of surface oxidation treatment on the dielectric properties of delignified material," *RSC Advances* 15(17), 12931-12939. https://doi.org/10.1039/d5ra01052g

Yao, H., Xiong, Y., Pickles, C., Hutcheon, R., Pahnila, M., Hagström, A., Fabritius, T., and Omran, M. (2025). "Dielectric properties of biomass by-products generated from wood and agricultural industries in Finland," *Bioresource Technology* 426, article 132319. https://doi.org/10.1016/j.biortech.2025.132319

Yardım, T., Demir, A., Allı, S., Allı, A., and Yücedağ, İ. (2020). "Investigation of the performance of poly (methyl-acrylate) as a gate dielectric in organic thin-film transistors," *J. Elec. Mater.* 49(6), 3830-3836. https://doi.org/10.1007/s11664-020-08090-1

Zelinka, S. L., Stone, D. S. and Rammer, D. R., (2007). "Equivalent circuit modeling of wood at 12% moisture content," *Wood and Fiber Science* 39(4), 556-565.

Zha, J.-W., Wang, S.-J., Dang, Z.-M., and Chen, G. (2021). "Polymer-based dielectrics with high permittivity for electric energy storage," *Nano Energy* 89, article 106438. https://doi.org/10.1016/j.nanoen.2021.106438

Zhou, J., Zhou, H., Hu, C., and Hu, S. (2013). "Measurements of thermal and dielectric properties of medium density fiberboard with different moisture contents," *BioResources* 8(3), 4185-4192.

Article submitted: August 14, 2025; Peer review completed: October 11, 2025; Revised version received and accepted: October 16, 2025; Published: July 14, 2026.
DOI: 10.15376/biores.21.3.8200-8225